THERMAL DECOMPOSITION ANALYSIS OF ROCKET MOTORS AND OTHER THERMAL PROTECTION SYSTEMS USING MSC.MARC-ATAS

Ted B. Wertheimer, MSC.Software (Palo Alto, USA)

Fabrice Laturelle, Snecma Propulsion Systems (Bordeaux, Fr.)

ABSTRACT

Design of solid rocket motors requires an extensive knowledge of the thermal behavior for reliability and optimization of the payload. Within a solid rocket motor, a complex thermo-chemical-aerodynamic process occurs. During the launch, the combustion of the solid propellant generates intense heat, often reaching 3600 K. This results in a thermal decomposition of the combustion chamber housing and the nozzle due to pyrolysis, and the ablation/erosion of the latter due to thermal, chemical, and mechanical processes. Additionally, within the engine, radiation occurs which is dependent upon the current geometry, and the amount of combustion that has occurred. Recent developments have let to the solution of these problems for both axisymmetric and three-dimensional geometries. Particular emphasis has been placed on the efficient calculation of the thermal radiation. This paper discusses the numerical simulation of the pyrolysis, surface energy inputs, thermal contact and radiation calculations.

INTRODUCTION

Snecma Moteurs, Rocket Motors Division, through its subsidiaries Europropulsion and G2P, is the prime contractor for developing the solid propellant rocket motors of Ariane 5 launchers and of the French deterrence force. Snecma Moteurs also develops thermal protection systems for reentry vehicles and bodies, and spatial probes.

What these products have in common is that some parts are subject to very high thermal fluxes (both convective and radiative), thermochemical oxidation by reactive chemical species, sometimes large mechanical and thermomechanical loads, and mechanical and chemical interactions with impacting liquid and solid particles. These loads have their origin in the high temperature, highly reactive and often particle laden surrounding flow generated either by the combustion of the fuel or by the speed of the vehicle. For instance, the nozzle and the internal thermal protection liners of a solid rocket motor can undergo fluxes up to 10 MW.m^{-2} and alumina particles impacts, during one or two minutes, from the flow produced by the combustion of the solid propellant. Some bodies on re-entry encounter thermal fluxes up to 100 MW.m-2.

To sustain such conditions, these motors and vehicles use advanced composite materials, such as carbon/carbon composites, carbon/phenolic composites, silica/phenolic composites,

ceramic matrix composites, and reinforced rubber-like materials as shown above. Among these materials, some are thermodegradable and undergo a chemical transformation known as pyrolysis producing decomposition gases and possibly brittle solid residue. Those materials and others that are not thermodegradable undergo surface recession, due to heterogeneous chemical reactions with the oxidizing chemical species of the surrounding flow, in which case we speak of thermochemical ablation or due to mechanical erosion by mechanical loads, which is often due to particle impacts.

The parts play a fundamental role for the thermal and mechanical integrity of the motor/vehicle for its safety, reliability, and performance. Hence, the temperature through the material, the thermo-poro-mechanical behavior induced, and the modifications of the geometry due to thermochemical ablation/mechanical ablation must be understood.

In the past, the convenient design and sizing was obtained by a large sequence of destructive full-scale motor tests. Now, the need for cost and design cycle reduction for solid rocket motors, due to severe concurrence on the market, leads to the requirement for more comprehensive and precise numerical models. This allows for the design of the motor with fewer tests, minimal material, and, perhaps, more cost effective material.

During the past 40 years, many people have dealt with the modeling of the behavior of these materials in such environments. This work has lead to comprehensive models, and numerous in-house developed software programs often dedicated to a single material modeling. The modeling of the behavior of a whole motor, with its nozzle and its combustion chamber coated by thermal protection during and after the combustion of the grain, often requires the use of four or five different simple software programs, each focused on a peculiar aspect of the problem. This software is often limited to one- or two-dimensional conditions. The use and maintenance of several aging software programs cost time and manpower.

Snecma Moteurs recognized that the general behavior of the different materials listed above could be described by a single theory with increasing levels of complexity. This offers the opportunity to implement some of these modeling levels in a single, general, multi-material software capable of 3-D analysis, replacing all the former in-house developed software programs, and capable of more comprehensive, precise, and user-friendly modeling.

Poro-thermal and ablative behavior of thermodegradable material

This paragraph focuses on the thermal aspects of the problem, and very little will be written on the associated poro-thermo-mechanical aspects. Nevertheless, the reader may keep in mind that the discussed pore pressure and thermal degradation of the material have tremendous effects on these aspects.

Consider the case of a carbon/phenolic material used as a thermal protection liner in solid rocket motors. Such a material is exposed to a high thermal flux and chemically reactive environment, thermal degradation occurs and its structure changes as shown.

Starting from the rear side of the material, we find first, a
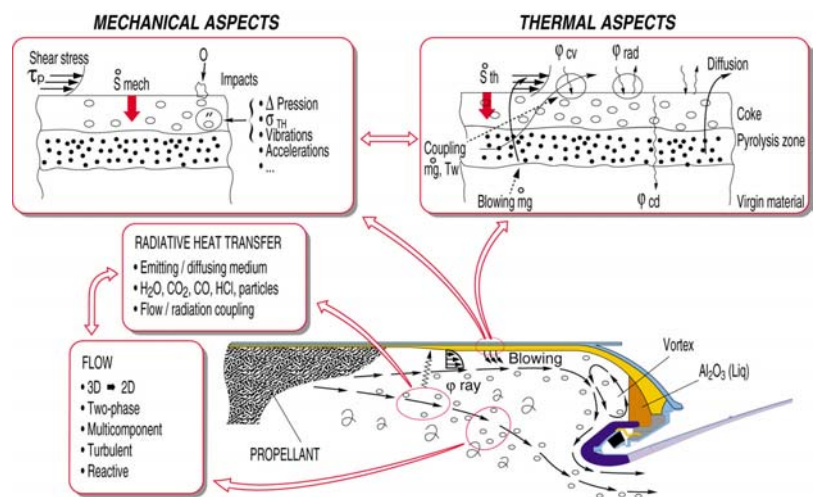
nondegraded low temperature zone, with original low porosity and permeability, where thermal evaporation of trapped chemical species as water occurs [1-2]. This produces a high internal pore pressure.

At higher temperature range (300°C – 600°C) for solid propulsion heating rate conditions, the primary pyrolysis chemical reactions occur, turning the long polymer chains constituting the resin matrix into high molecular weight gaseous chemical species, and a

carbonaceous solid residue [3-5]. In this zone, a pore pressure also develops although the porosity and the permeability of the material are increasing rapidly due to the loss of solid mass. The solid density decreases.

This pore pressure induces a flow of the rather cool gaseous products through the residue toward the heated surface upstream the heat flux, producing a cooling internal convection effect.

As higher temperatures are encountered (1000°C-1400°C), the thermal cracking of the gaseous phase continues further, generating less molecular weight chemical species. Depending on the local conditions, the gas can be in a state of chemical equilibrium or disequilibrium [6-7]. Besides these gas/gas reactions at still higher temperatures, some other reactions and transformations may occur. For instance, a graphitization of the residue can sometimes be observed. Another important phenomenon is the so-called coking [8]. The flowing gaseous products are introducing too much carbon than the chemical equilibrium allows at these temperatures. Hence, a solid carbon deposit in the residue is observed, which can reduce the porosity and the permeability, and again increase the local density left by the primary pyrolysis. This latter effect increases the resistance of the material to the thermochemical ablation discussed below.

Just below the heated surface, where the temperature can reach the range of 2500°C-2800°C, the thermodynamic conditions and the chemical species available in the internal gas flow change the direction of heterogeneous gas/solid reactions. There, instead of a carbon being deposited by coking, the carbon of the residue is now turned into gaseous species. At the surface itself, the external flow around the part contains similar gaseous chemical species, such as water vapor and carbon dioxide. Globally, the heterogeneous chemical reactions between these species at the solid surface and just below lead to a mass loss. This is known as thermochemical ablation and results in a recession of the surface. Numerous papers and books are devoted to this phenomenon, for instance [3,9-15]. The process can be controlled either by chemical kinetics or by the rate of diffusion of the chemical species through the boundary layer of the external flow, depending on the local temperature and flow conditions.

Ablation absorbs a great quantity of energy, as the water evaporation and pyrolysis reactions do. Another influence on the heat transfer reduction is due to the blowing of the boundary layer of the external flow by the gaseous products of thermal decomposition and ablation. With the above-mentioned internal convection cooling effect, these phenomena explain why these materials exhibit excellent thermal insulation properties.
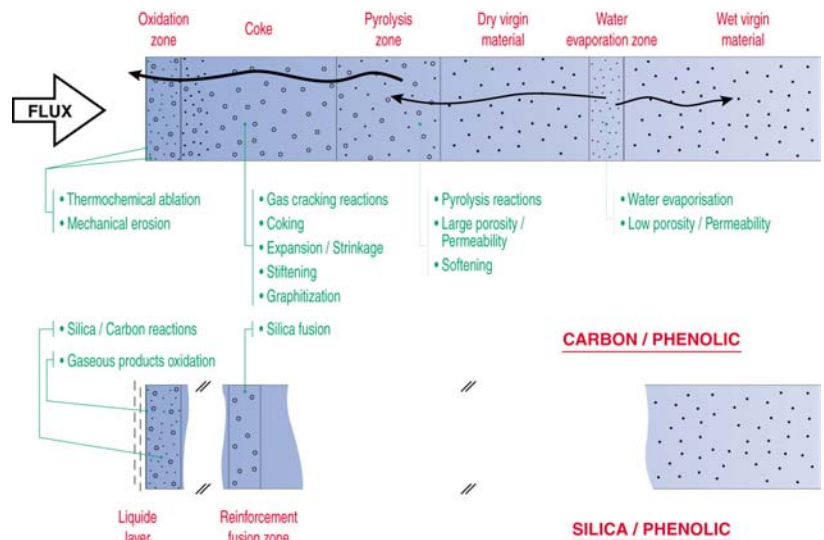
Besides these chemical processes, if the residue is brittle, mechanical or dynamical loads can erode it [12-13]. Mechanical erosion is important for instance in the case of rubber-like materials used as internal thermal protection for the combustion chamber of the solid rocket motor [16].

As the combustion of solid propellant produces liquid or solid alumina particles, these latter can impact the walls of the motor and cause additional thermochemical ablation or mechanical erosion depending on the impact conditions. Impacts are also encountered in other applications of these materials [13].

In the case of a silica/phenolic composite, the process can be more complex, with additional phenomena such as reactions between the silica constituting the reinforcement and the carbon produced by the pyrolysis, fusion of the silica reinforcement, re-oxidation at the surface of some gaseous silicon oxide into liquid products [7,17-19]. On the contrary, with nonthermodegradable and tuff materials such as carbon/carbon composites, only the surface thermochemical ablation is relevant [11].

Physical models, numerical methods, and results for ablation and pyrolysis

2.1 Physical models

Many different models with increasing complexity can be considered concerning the surface energy balance under thermochemical ablation and mechanical erosion conditions. For instance, the ablation rate and the surface temperature may be imposed by the user from test results, the popular concept of heat of ablation may be used, or a full energy balance such as proposed by Kendall, Rindal and Bartlett [9]. Some different models will be available in MSC.Marc-ATAS, but only the latter is discussed here.

The full surface energy balance (SEB) is required to determine the conductive flux entering the material, the surface temperature, and the surface recession velocity during an ablation/erosion process, from the external flow configuration. Besides the conductive flux, the SEB takes into account convective heat flux with a possible blowing effect due to mass injection, a radiative balance, an enthalpy flux due to molecular diffusion of the chemical species in the boundary layer, three enthalpy fluxes associated with the mass transfer due to thermochemical ablation by gases and thermal internal decomposition, two enthalpy fluxes associated with thermochemical ablation, and a mechanical erosion by liquid or solid particles impacts, and possible removal of liquid phases formed at the surface.

The surface energy balance (SEB) allows one to obtain the recession due to thermochemical ablation by gases or particles. The other part of the surface recession, due to the mechanical erosion, is calculated by other means. Both contributions are summed to obtain the total surface recession.

The SEB is coupled with the heat transfer into the material by the conductive heat flux, and with the mass flow rate towards the surface due to thermal decomposition gases generated inside the material.

The following figure illustrates the in-coming and out-going flux in a control volume at the surface.
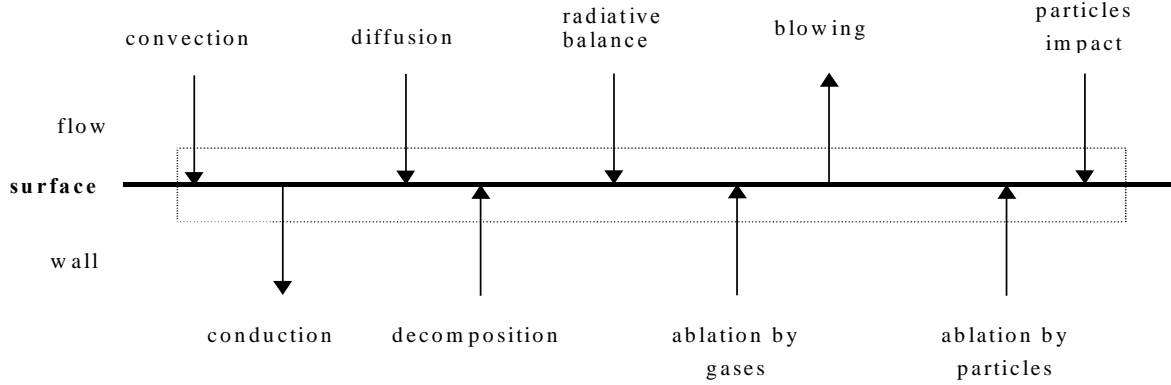
The adopted expression for the SEB is:

$$\lambda_s^* \frac{\partial T}{\partial n}\bigg|_{surface} = \alpha_H \left(H_{rec} - H_e^{T_S}\right) - (\rho v)_w H_w + \alpha_M \sum_i \left(Z_{ie}^* - Z_{is}^*\right) H_i^{T_S} + \dot{m}_{s,th,g} H_s + \dot{m}_g H_g$$

$$+ f_{th,p} \sum_j G_{th,p,j} \dot{m}_{p,j} \Delta H_{r,p,j} - \sum_l \dot{m}_l H_l + \Phi_{rad,absorbed} - \Phi_{rad,emis}$$

The reader should refer to classical papers and books on ablation for further insight in the SEB [9,14-15]. A set of so-called classical G-Law model is used for modeling thermochemical ablation by impacts of several different families of particles.

Both gases and impacting particles contribute to a chemical ablation that can be expressed by:

$$\dot{s}_{th} = (\dot{m}_{s,th,g} + \dot{m}_{s,th,p})/\rho_S, \qquad \text{with} \quad \dot{m}_{s,th,g} = f_{th,p} \sum_j G_{th,p,j} \dot{m}_{p,j}$$

where $\dot{s}_{th}$ is the recession velocity due to chemical reactions and ρ_S the solid density.

Besides this thermochemical ablation, mechanical erosion can occur:

$$\dot{s} = \dot{s}_{th} + \dot{s}_{mec}$$

Until now, the development has dealt with level-1 and level-2 models discussed above, for the modeling of internal behavior. This paper focuses on the latter in a simplified form, and nothing is written on water evaporation and coking.

In the level-2 model, the decomposition of the material is represented by two equations: the mass balance gives as a result the mass flow rate of the pyrolysis gas and the solid density, and the energy balance, which takes into account the contribution of the pyrolysis, through which one obtains the temperature. Moreover, the concept of geometrical streamlines explained above is used.

The expression for the mass balance is:

$$\nabla . \dot{m}_g = -\frac{\partial \hat{\rho}_{s,p*}}{\partial t}$$

where $\dfrac{\partial \hat{\rho}_{s,p*}}{\partial t}$ is the rate of decomposition of the solid material, and $\dot{m}_g$ the mass flow rate of pyrolysis gas.

As the material can be composed by several components, the rate of decomposition is a sum of Arrhenius laws.

$$\frac{\partial \hat{\rho}_{s,p}}{\partial t} = \sum_{j=1}^{n} -\Gamma_j B_j' \exp\left(-T_{aj}/T\right) \hat{\rho}_{svj} \left(\frac{\hat{\rho}_{spj} - \hat{\rho}_{scj}}{\hat{\rho}_{svj}}\right)^{\psi_j}$$

where $\hat{\rho}_{spv}$ is the density of the virgin material, and $\hat{\rho}_{spc}$ is the density of the charred material, and $\hat{\rho}_{spj}$ is the current density of the jth component of the solid.

The mass balance is integrated along the geometrical streamlines:

$$\iint_{\partial s \times \partial x} \frac{\partial \dot{m}_g}{\partial x} \, dx \, ds = \iint_{\partial s \times \partial x} -\frac{\partial \hat{\rho}_{s,p}}{\partial t} \, dx \, ds \ .$$

This leads to the following numerical scheme to calculate the mass flow rate of the pyrolysis gas:

$$s(x_k) \dot{m}_g(x_k, t^{n+1}) = s(x_1) \dot{m}_g(x_1, t^{n+1}) - 0.5 \sum_{i=2}^{k} (x_i - x_{i-1}) \left(\frac{\partial \hat{\rho}_{s,p*}(x_i)}{\partial t} s(x_i) + \frac{\partial \hat{\rho}_{s,p*}(x_{i-1})}{\partial t} s(x_{i-1})\right)$$

As quoted above, the solid and the gas are assumed to be in thermal equilibrium leading to a one-temperature model. The energy balance includes a convective term due to the motion of the pyrolysis gas in the porous media and an enthalpic term [3]. It is written as:

$$\hat{\rho}_s c_p \frac{\partial T}{\partial t} + c_{pg} \dot{m}_g . \nabla T = \nabla . \left(\lambda^* \nabla T\right) + \frac{\partial \hat{\rho}_{s,p*}}{\partial t} \left(H_{g,p} - \overline{H}_{s,p,vc}\right)$$

where enthalpies are absolute enthalpies, defined by $H = \Delta H_f^0 + h = \Delta H_f^0 + \int_{T_0}^{T} c_p dT$ and where ($\overline{H}_{g,p}$ - $\overline{H}_{s,p,vc}$) represents some kind of 'heat of pyrolysis', with

$\overline{H}_{s,p,vc} = \dfrac{\hat{\rho}_{s,p,v*} H_{s,p,v*} - \hat{\rho}_{s,p,c*} H_{s,p,c*}}{\hat{\rho}_{s,p,v*} - \hat{\rho}_{s,p,c*}}$ being an effective enthalpy for the degrading solid.

The energy equation is solved in the standard fashion by finite elements in MSC.Marc.

2.2 Material behavior

During the pyrolysis, the material undergoes a phase transformation from the outside surface to the interior region as shown below. It is assumed that coking takes place in completely pyrolysed material. The effective material properties are defined as:

$$\lambda^* = \left(1 - \xi_p\right)\lambda_v + \xi_p(1 - \xi_c)\lambda_c + \xi_p\xi_c\lambda_{cd}$$

which relates the effective conductivity λ^* to the virgin λ_v, charred λ_c and coked conductivity λ_{cd}, using the rate of pyrolysis ξ_p and the rate of coking ξ_c. Hence, the user need to define the material properties in three states, all of which may be anisotropic and temperature dependent. To facilitate this, a new THERM-PORE option has been introduced to allow these properties along with their respective enthalpy of formation. A new option has also been introduced to allow the user to associate a table (MSC.Patran Field) to any material property. These tables may have up to four independent variables to permit general spatial variation without the need of user subroutines. This capability has been generalized to support all of the material properties, boundary conditions, and contact data in MSC.Marc.

Numerical methods

3.1 Ablation analysis

As previously discussed an important aspect of modeling thermal protection systems is examining the consequences of surface recession by ablation. Building on the pioneering work in MSC.SuperForm automatic remeshing procedures have been developed. In conventional heat transfer analysis, mechanical displacements are not considered. In these analyses, a zero displacement has been introduced, except at the surface nodes where recession is allowed. The surface recession rate may be due to one of the sources discussed above or may be a simple user-defined function. The recession model and the relevant surface are defined in a new RECEDING SURFACE option. This recession rate is evaluated at the surface integration points and a consistent nodal displacement is obtained. The next step is to determine when remeshing is required. For manufacturing analysis, the common criteria are based upon mesh distortion as the finite element mesh degenerates with distortion. In these ablation problems, where, initially, very thin elements are used, these distortion criteria were determined to be inadequate. Rather, a criteria based upon the percentage reduction in element thickness in the direction of the streamline was developed. Furthermore, the time step is adaptively controlled among other restraints so that the surface recession distance per time step must be less than a critical dimension. It should be noted that while the element aspect ratio often is greater than 50:1, this does not lead to computational difficulties for heat transfer analysis.

Initially it was felt that mesh generators, such as the advancing front or Delauney, could be applied to remesh the region after ablation occurred. But, based upon the requirements imposed due to the streamline integration technique and for the mesh requirements to accurately capture high thermal gradients, these methods proved fruitless. Rather, two methods of remeshing have been implemented: mesh relaxing and mesh shaving. In the first technique, the number of elements remains the same and the nodal coordinates are perturbed in the direction of the normal. This results in equal spacing through the thickness. In the second technique, the outside element is stripped off when it becomes arbitrarily thin. The

other elements are left undisturbed. Depending on whether the recession is uniform over the surface, an element will be either fully removed or degenerated to a triangle, followed by subsequent removal. In either case, after the mesh is modified, the elemental data is mapped (rezoned) to the new integration points. A similar process is performed for streamline data. When using such techniques, care must be exercised when viewing conventional results for the history of a nodal quantity is dubious, as the node does not represent a constant material particle. For this reason, special tracking options have been developed.

Because the shaver mesher changes the element and node numbers that are on the exterior surface, a new geometry based boundary capability was added to MSC.Marc. Using this procedure, all boundary conditions (prescribed temperatures, fluxes, convection) may be applied to a point, curve (2-D), or surface (3-D). The conventional finite element entities (nodes, element-faces) are attached to the geometric entities. As the finite element model changes, the new mesh is automatically associated with the geometry, and boundary conditions are correctly applied. This treatment of boundary conditions also facilitates improved connectivity to CAD in the future. The new boundary condition procedure works in conjunction with tables to allow maximum flexibility.

3.2 Streamline Definition for level-2 model

In the numerical procedure outlined above, the flow rate is integrated along geometrical streamlines to represent simplified one-dimensional fluid flow. The program, based upon the assumption that a regular but not necessarily uniform mesh is provided for two- or three-dimensional analysis, automatically calculates the streamlines. Certain quantities are evaluated at the stream integration points (SIP), shown in the figure below. Unfortunately, finite elements impose the requirements that these quantities are at the conventional integration points to evaluate the material properties, and other source terms. Hence, first a weighted nodal average of the extrapolated quantities are obtained followed by interpolating to the conventional integration points. Because of the large number of elements through the thickness, this procedure did not show any loss in accuracy.

Regular Mesh

SIP) Streamline Integration Point
CIP) Conventional Integration Point
SFIP) Surface Integration Point
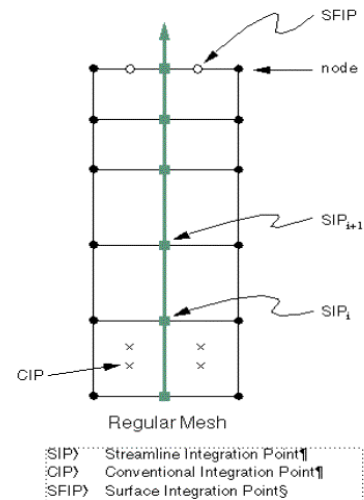
Results

An example of ablation calculation is given below, comparing MSC.Marc-ATAS results with a previously developed Snecma Moteurs in-house software program. Using the same boundary conditions, the surface recession and the temperature inside the material are similar for both programs.

Temperature field in the material for different times while ablation .
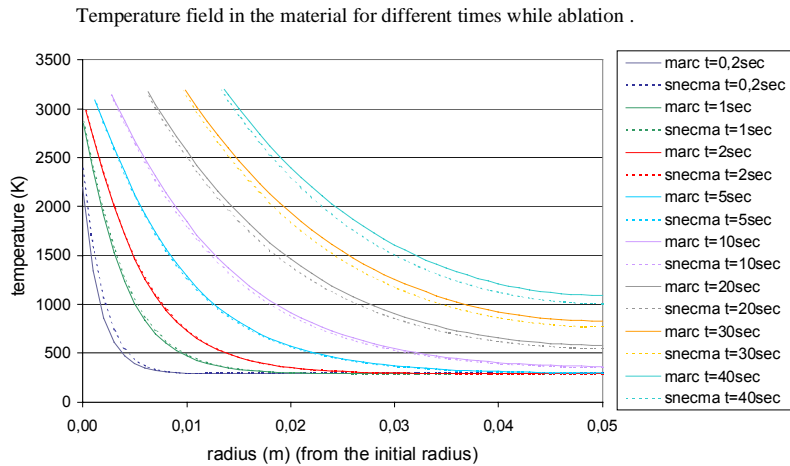
Below is another example of calculation with pyrolysis but no ablation. A comparison is made with another older in-house developed Snecma Moteurs software program. The temperature fields inside the material are in good correlation.

Comparison of the temperature between the Snecma code and Marc (MSC) along the material at different times
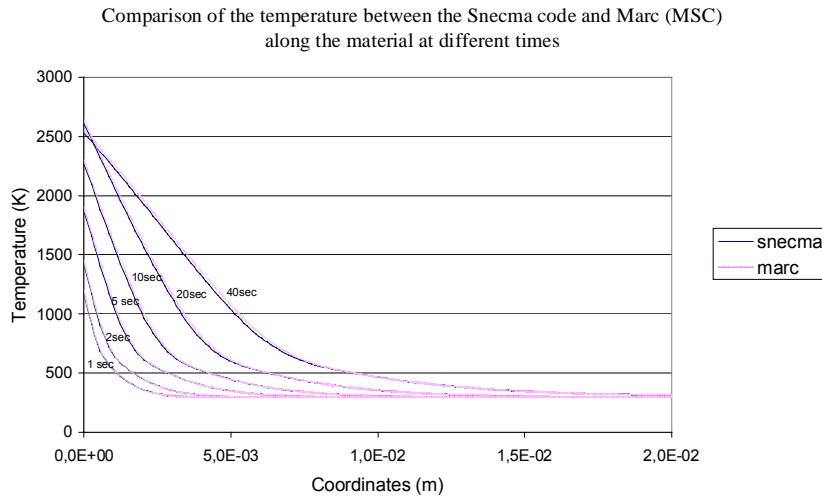
During the process, the material is pyrolysed, and we can see the pyrolysis progressing and the density decreasing inside the material.

Comparison of the density field inside the material between the Snecma code and Marc (MSC)
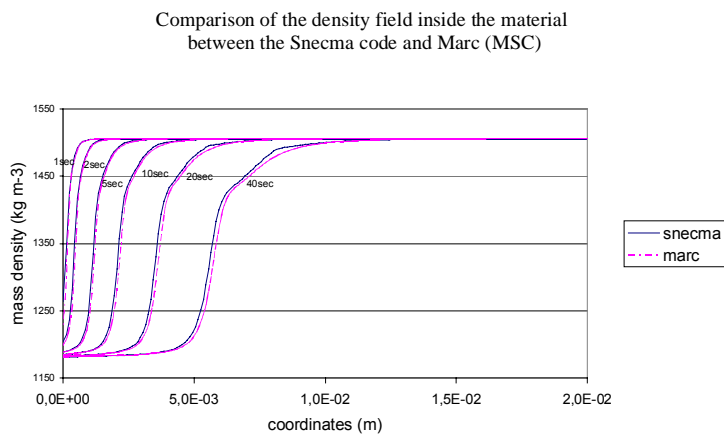
The thermal decomposition produces gases that are assumed to flow out instantaneously. The gas quantity created is summed along the streamlines, and we obtain the following curve that shows the mass flow rate of the gas arriving at the surface during the process.

Comparison of the mass flow rate at the exterior surface between the Snecma code and Marc (MSC)
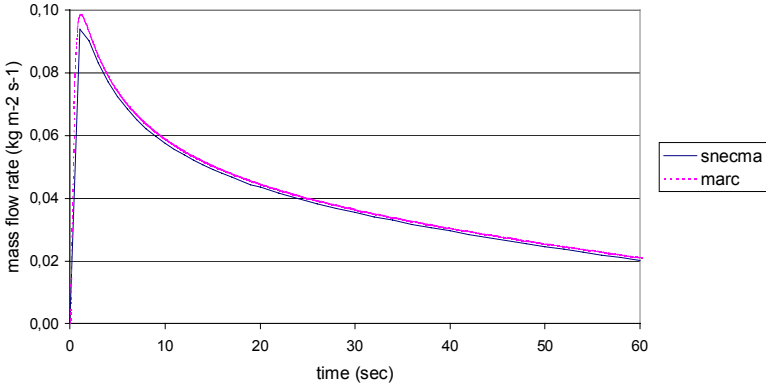
These examples are based on one-dimensional configurations and used for the validation of MSC.Marc-ATAS. Nevertheless, as quoted above, this latter allows the program to deal with general multi-dimensional configuration not possible for the older level-2 software, and includes the level-3 model for which no software is currently available.

As an example of two-dimensional behavior the thermal solution of a simplified reduction area was obtained. The surface energy input is dependent upon the distance along the flow, and the current area relative to the throat area. The analysis was performed twice, to evaluate the two remeshing techniques required due to ablation.
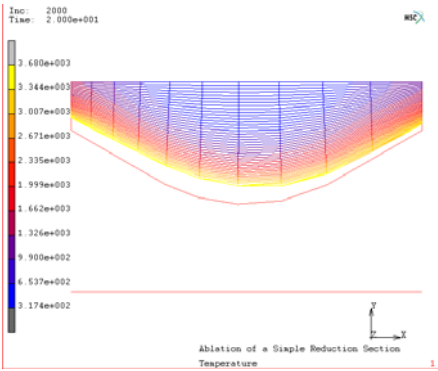
Shaver Mesher
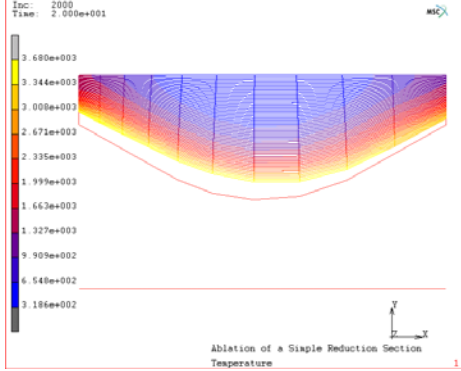
Relax Mesher

Thermal Contact

A solid rocket motor is built from many different parts, constituted by several materials having very different thermal properties, and, by design, there are some gaps allowing the thermomechanical expansion to occur without failure. To simplify the model of these discrete parts, a new thermal contact option has been added to MSC.Marc. This option may also be successfully be used to model assemblies of noncongruent meshes. The thermal contact behavior option behaves in a similar manner to the contact option in thermal-mechanically coupled analyses, but with several enhancements. The flux across a surface is based upon three potential states:

No contact – distance from nodes to another surface dX > dnear :

$$q= h_{cv}* (T_1-T_{env})$$

Near contact – distance from node to another surface dcontact < dX < dnear

$$q=h_{cv}*(T_2-T_1) + h_{nt}* (T_2-T_1)^{ent} + * *(T_2^4-T_1^4) + (h_{ct} -(h_{ct}-h_{bl})*dX* (T_2-T_1)/dnear$$

True contact – distance from node to another surface dX < dcontact

$$q=h_{ct}*(T_2-T_1)$$

Where h_{cv} is the convective coefficient, h_{nt} is the natural coefficient, h_{bl} is the convective coefficient at the boundary layer, and h_{ct} is the contact coefficient. All coefficients may be spatially and temporally dependent. T_1 and T_2 are the temperatures at surface 1 and 2, respectively, while T_{env} is the temperature of the environment. For near contact, a simplified radiation model is available. The assumption is that the radiation is between the two closest surfaces, with no shadowing or other geometric effects. This capability is available for both two- and three-dimensional models.

Radiation

Radiative thermal heating is a significant contributor to the thermal process and leads to complexity in the numerical simulations. Interior to the rocket motor, the environment transitions from a highly gaseous and particle filled medium to a near vacuum during the combustion and post combustion periods. Because of ablation, the geometric changes may have an influence on the view factors, and need to be recalculated if the finite element mesh changes. MSC.Software has embarked on enhancing and modularizing the view factor calculation to be more computationally efficient. Currently, the following view factor procedures are employed at MSC:

Finite Difference (MSC.Nastran)

Contour Integrations   (MSC.Nastran and MSC.Thermal)

Gaussian Integration   (MSC.Nastran)

Monte Carlo   (MSC.Marc)

Regardless of the method used to calculate the view factors there are two consequences:

1. The number of view factors becomes large, growing quadratically with the number of radiating surface.

2. The subsequent calculation in the analysis program is dependent upon the number of view factors calculated.

The number of view factors is reduced because of shadowing effects, but depending upon the procedure used to calculate the view factors, this may lead to higher computational costs in calculating them. Because of shadowing, sparse storage techniques are beneficial .

Using finite difference, contour integral, Gaussian integration or direct integration the number of operations increases quadratically with the number of radiating surfaces. All of these procedures (combined with adaptive approaches or refined meshes) can produce accurate

results, but at a clear computational cost. The Monte Carlo method the computational cost increases linearly with the number of radiating surfaces, and increases linearly with the number of emitting rays. This clearly is beneficial for large models. The problem with the Monte Carlo method is that a large number of rays may be necessary to achieve accurate results (for example if thin cavities exist).

A new procedure has been developed that is a pixel based modified hemi-cube method. This is based upon the work of Willmott [24] and is available for planar,axisymmetric and three-dimensional geometries for either continuum of shell elements. Multiple symmetry planes and cyclic symmetry may be included. The advantage of this method is that the computational costs are linearly dependent on the number of radiating surfaces and linearly dependent upon the number of pixels. The accuracy is dependent upon the number of pixels chosen, and the size/shape of the cube. It is advantageous over the Monte Carlo method in that greater accuracy may be obtainted at a lower cost.. This is because the number of pixels is less than the number of rays required, and the computational cost in the kernel is less.

The foundation of radiation is based upon radiation being received from multiple directions and/or being emitted in multiple directions. This leads to the concept of a hemisphere, where one considers an element being projected onto the hemisphere as shown in Figure 1.
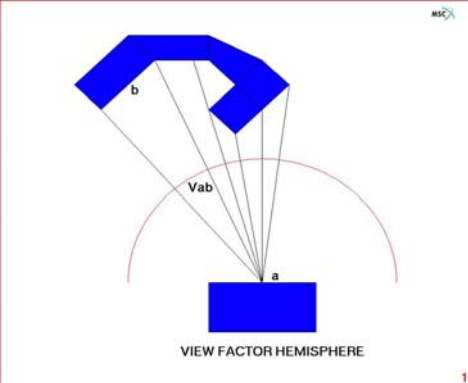
Figure 1
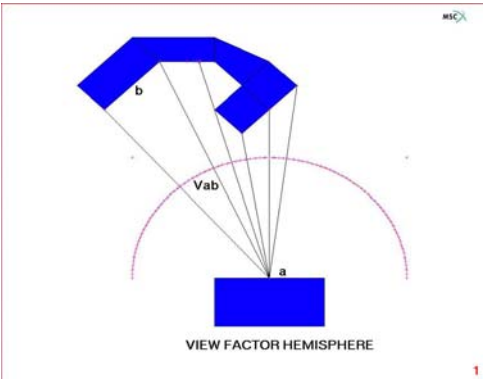
Figure 2

This geometric projection can be "easily" calculated for 2-D or axisymmetric, but is problematic in 3-D. To overcome this problem of exact projections one can consider dividing the hemisphere into pixels as shown in Figure 2, and the simple "count" the pixels. This procedure is easier to implement in 3-D, though it is still expensive. As an alternative one can approximate the hemisphere with a hemi-cube as shown in Figure 3.
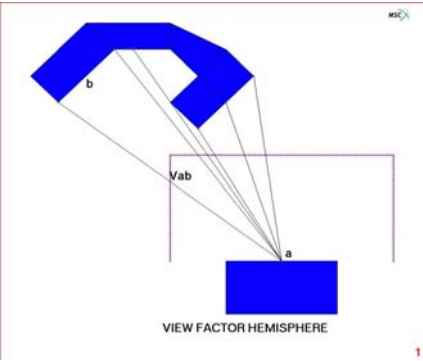
Figure 3
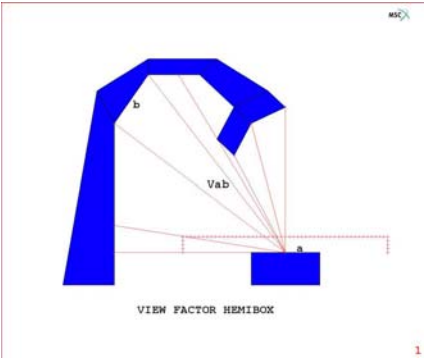
Figure 4

Using the hemi-cube method is less expensive, but is still difficult around the edges, and especially the corners in 3-D. One way to reduce this problem is to change the dimensions of the box, such that there is a smaller possibility that leakage out of the sides is important and then simply neglect this. This is shown in Figure 4, where a hemi-box now replaces the hemi-cube. To retain accuracy, one must select a good dimension of the box, and as the space is now biased, an equally spaced pixel grid will lead to inaccuracies. To overcome this problem a hemi-plane will be used with non-equally spaced pixels, such that the weight of each pixel is the same. This is shown in Figure 5.
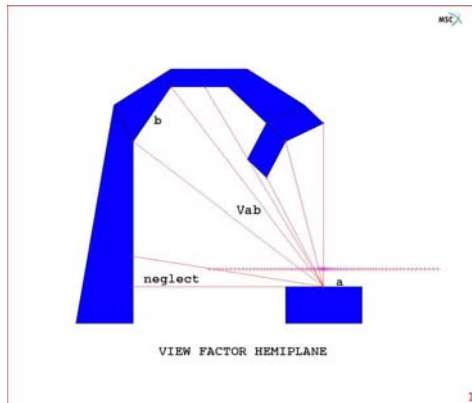
Figure 5

There are five reasons why it may be necessary to recalculate view factors in a heat transfer or coupled thermal-mechanical analysis:

1. Orbital motion is to be modeled.

2. Ablation in the model results in geometric changes and possibly changes in the model topology, and or changes in the shadowing.

3. High temperature cradients activate the local remeshing procedure which changes the topology.

4. Large displacements occur, which result in the change of geometric view factors.

5. Large strains occur that require remeshing in the model, such as in manufacturing.

As an example a simplified rocket motor was modeled with an artificial hot spot inducing a non-uniform thermal distribution that resulted in a burn through of the wall. This model was designed to test the new capabilities, and does not reflect a real structure. In the analysis 1000 increments were used to model 10 seconds, and the viewfactors were calculated 101 times.

Other applications

The study of pyrolysis and ablation, while critical for the rocket and reentry vehicle industry, has important value to other industries as well. The key common denominator is the presence of high fluxes and potential thermal-chemical degradation of the material. We observe these phenomena every morning when we make toast. The same technology is applicable to furnaces and other fire retardant insulation. Aspect of ablation are applicable in disk brakes, tire wear, gears, and potentially machining applications. Laser cutting exhibits many of the same physical phenomena that may be modeled using this technology.

Conclusions

The status of the development of the ATAS capabilities in MSC.Marc has been discussed. Excellent correlation has been found with previously developed simple modeling tool. The formulation incorporated in MSC.Marc will have far greater generality, allowing simulation of phenomena that was previously intractable. This will lead to reducing the time associated with design and in building and testing costly prototypes. Also, the use and maintenance of a single thermal software program with user-friendly inputs, plus being capable of coupled thermal/thermomechanical coupled analyses, will save time and money compared to the use of several older purely thermal software programs.

References

[1]   H.L.N. Mc Manus, G.S. Springer
        High temperature thermomechanical behavior of carbon-phenolic and carbon-carbon composites, I. Analysis.
        J. Composite Materials, Vol. 26, No. 2, pp. 207-229, 1992.

[2]   Y. Wu, N. Katsube
        Balance laws for decomposing carbon-phenolic composites with moisture.
        AIAA Paper 94-1581, AIAA/ASME/ASCE/AHS/ASC 35th Structures, Structural Dynamics and Materials Conference, 1994.

[3]   C.B. Moyer, R.A. Rindal
        An analysis of the coupled chemically reacting boundary layer and charring ablator. Part II. Finite difference solution for the in-depth response of charring materials considering surface chemical and energy balances.
        NASA CR-1061, June 1968.

[4]   A.D. Baer, J.H. Hedges, J.D. Seader, K.M. Jayakar, L.H. Wojcik
        Polymer pyrolysis over a wide range of heating rates.
        AIAA J., Vol. 15, No. 10, pp. 1398-1404, October 1977.

[5]   K.A. Trick, T.E. Saliba, S.S. Sandhu
        A kinetic model of the pyrolysis of phenolic resin in a carbon / phenolic composite.
        Carbon, Vol. 35, No. 3, pp. 393-401, 1997.

[6]   G.C. April, R.W. Pike, E.G. Del Valle
        Modeling reacting gas flow in the char layer of an ablator.
        AIAA J., Vol. 9, No. 6, pp. 1113-1119, June 1971.

[7]   G. Darmon, D. Balageas
        Transferts de chaleur et de masse dans un matériau composite pyrolysable.
        Revue Générale de Thermique, No. 262, pp. 197-206, avril 1986.

[8]   B. Laub
        The Apollo heatshield. Why performance exceeded expectations.
        Int. Symposium Atmospheric Reentry Vehicles and Systems, Arcachon,
        March 16-18, 1999.

[9]   R.M. Kendall, R.A. Rindal, E.P. Bartlett
        A multicomponent boundary layer chemically coupled to an ablating surface.
        AIAA J., Vol. 5, No. 6, pp. 1063-1071, June 1967.

[10]   J.W. Schaefer, H. Tong, R.J. Bedard
        Kinetic reaction rates for consumption of pyrolytic graphite.
        AIAA Paper 74-1056, AIAA/SAE 10th Propulsion Conference, San Diego,
        October 21-23, 1974.

[11]   K.K. Kuo, S.T. Keswani
        A comprehensive theoretical model for carbon/carbon composite nozzle recession.
        Combustion Science and Technology, Vol. 42, pp. 145-164, 1985.

[12]   G.B. Spear
        The role of chemical reactions and mechanical erosion in aerothermal modeling
        of external insulations.
        AIAA Paper 90-1868, AIAA/SAE/ASME/ASEE 26th Joint Propulsion Conference,
        Orlando, July 16-18, 1990.

[13]   B.C. Yang, F.B. Cheung, J.H. Koo
        Numerical investigation of thermo-chemical and mechanical erosion of ablative
        materials.
        AIAA Paper 93-2045, AIAA/SAE/ASME/ASEE 29th Joint Propulsion Conference
        and Exhibit, Monterey, June 28-30, 1993.

[14]   B. Laub, R.A.S. Beck
        Characterization and modeling of low density TPS materials for recovery vehicles.
        SAE Technical Paper Series 941368, 24th International Conference on
        Environmental Systems and 5th European Symposium on Space Environmental
        Control Systems, Friedrichshafen, June 20-23, 1994.

[15]   F.S. Milos, Y.K. Chen
        Comprehensive model for multicomponent ablation thermochemistry.
        AIAA Paper 97-0141, AIAA 35th Aerospace Science Meeting & Exhibit, Reno,
        January 6-9, 1997.

[16]   F. Laturelle et al.
        Ablation des protections thermiques internes dans les propulseurs à propergol
        solide. Colloque Ecoulements Propulsifs dans les Systèmes de Transport Spatial,
        Bordeaux, 11-15 septembre 1995.

[17]   F.E. Romie
        Carbon-silica reaction in silica-phenolic composites.
        AIAA J., Vol. 5, No.8, pp. 1511-1513, August 1967.

[18]   C.L. Hsieh, J.D. Seader
        Surface ablation of silica-reinforced composites.
        AIAA J., Vol. 11, No. 8, pp. 1181-1187, August 1973.

[19]   J.B. Henderson, M.R. Tant
        A study of the kinetics of high-temperature carbon-silica reactions in an ablative
        polymer composite.
        Polymer Composites, Vol. 4, No. 4, pp. 233-237, 1983.

[20]   R.L. Potts
        Application of integral methods to ablation charring erosion. A review.
        J. Spacecraft and Rockets, Vol. 32, No. 2, pp. 200-209, March-April 1995.

[21]   R.M. Sullivan
        A coupled solution method for predicting the thermostructural response of
        decomposing, expanding polymeric composites.
        J. Composite Materials, Vol. 27, No. 4, pp. 409-434, 1993.

[22]   Y. Wu, N. Katsube
        A thermomechanical model for chemically decomposing composites-I. Theory.
        Int. J. Engineering Science, Vol. 35, No. 2, pp. 113-128, 1997.

[23]   J. Florio Jr., J.B. Henderson, F.L. Test, R. Hariharan
        A study of the effects of the assumption of local-thermal equilibrium on the overall
        thermally-induced response of a decomposing, glass-filled polymer composite.
        Int. J. Heat and Mass Transfer, Vol. 34, No. 1, pp. 135-147, 1991.